Involvement of recoverin C-terminal segment in recognition of the target enzyme rhodopsin kinase

Evgeni Zernii, Konstantin Komolov, Sergei Permyakov, Tatiana Kolpakova, Daniele Dell'Orco, Annika Poetzsch, Ekaterina Knyazeva, Ilya Grigoriev, Eugene Permyakov, Ivan Senin, et al.

INVOLVEMENT OF RECOVERIN C-TERMINAL SEGMENT IN RECOGNITION OF THE TARGET ENZYME RHODOPSIN KINASE

Evgeni Yu. Zernii[§1], Konstantin E. Komolov[ǂ§1,2], Sergei E. Permyakov[‖], Tatiana Kolpakova[§], Daniele Dell'Orco[ǂ], Annika Poetzsch[ǂ], Ekaterina L. Knyazeva[‖], Ilya I. Grigoriev[§], Eugene A. Permyakov[‖], Ivan I. Senin[§], Pavel P. Philippov[§] and Karl-Wilhelm Koch[2ǂ]

§ A.N. Belozersky Institute of Physico-Chemical Biology, M.V. Lomonosov Moscow State University, 119991 Moscow, Russia
ǂ Biochemistry group, Department of Biology and Environmental Sciences, University of Oldenburg, D-26111 Oldenburg, Germany
‖ Institute for Biological Instrumentation of the Russian Academy of Sciences, Pushchino, Moscow region 142290, Russia

[1] Both authors contributed equally to this work.
[2] to whom correspondence should be addressed:
Phone: +49 441 7983674, e-mail: konstantin.komolov@uni-oldenburg.de
Phone: +49 441 7983640, e-mail: karl.w.koch@uni-oldenburg.de

Running title: recoverin and rhodopsin kinase target recognition

Neuronal calcium sensor (NCS) proteins belong to a family of calmodulin-related EF-hand Ca^{2+}-binding proteins which in spite of a high degree of structural similarity, are able to selectively recognize and regulate individual effector enzymes in a Ca^{2+}-dependent manner. NCS proteins vary at their C-termini that could therefore serve as structural control elements providing specific functions like target recognition or Ca^{2+}-sensitivity. Recoverin, an NCS protein operating in vision, regulates the activity of rhodopsin kinase, GRK1, in a Ca^{2+}-dependent manner. We investigated a series of recoverin forms that were mutated at the C-terminus. Using pull down assay, surface plasmon resonance spectroscopy and rhodopsin phosphorylation assay, we demonstrated that truncation of recoverin at the C-terminus significantly reduced the affinity of recoverin for rhodopsin kinase. Site directed mutagenesis of single amino acids in combination with structural analysis and computational modeling of recoverin-kinase complex provided insight in the protein-protein interface between kinase and the C-terminus of recoverin. Based on these data we suggest that F3 from the N-terminal helix of rhodopsin kinase and K192 from the C-terminal segment of recoverin form a cation-π interaction pair which is essential for target recognition by recoverin. Taken together, our study revealed a novel rhodopsin kinase binding site within C-terminal region of recoverin and highlights its significance for target recognition and regulation.

The abbreviations used are: NCS, neuronal calcium sensor; GCAP, guanylate cyclase-activating protein; KChiP, K^+-channel interacting protein; PCR polymerase chain reaction; RK, rhodopsin kinase; N-RK, N-terminal region of rhodopsin kinase; ROS, rod outer segments; SPR, surface plasmon resonance; GST, glutathione-S-transferase; PDB, Protein Data Bank, ZD*i*, docking score index; ZD-s, average docking scores.

Key words: NCS, GRK, ternary protein complex, cation-π interaction, visual phototransduction, calcium feedback mechanism

INTRODUCTION

Various aspects of neuronal function are regulated by changes in intracellular Ca^{2+}-concentration. The intensity and duration of Ca^{2+}-signals can trigger the activation of different Ca^{2+}-pathways leading to specific physiological effects [1]. Eventually the large diversity of Ca^{2+}-regulated events is the result of the action of Ca^{2+}-sensor proteins, which transform Ca^{2+}-signals into a wide range of cellular responses. The specificity of such transduction pathways depends on the affinity of the Ca^{2+}-sensor for Ca^{2+}, on the intracellular localization of the Ca^{2+}-sensor and on the ability of the Ca^{2+}-sensor to interact with effector enzymes [2]. Ca^{2+}-sensor proteins contain specific structural elements, such as EF-hand motifs or C2-domains that recognize and bind Ca^{2+} in a highly sensitive and specific manner [3, 4]. Binding of Ca^{2+}

triggers conformational changes in the protein enabling the protein to specifically modulate the activity of intracellular effector proteins (several Ca^{2+}-sensors can modulate the activity of the target proteins in Ca-free (apo-) form) [5].

While some of the known Ca^{2+}-sensors are ubiquitous, the expression of others is restricted to certain tissues or cell types. The most common ubiquitous Ca^{2+}-sensor is calmodulin that is widely expressed and regulates a large variety of targets. NCS proteins have a more restricted expression pattern and repertoire of target proteins. This protein family can be divided into five groups based on structural and functional similarities: recoverins, visinin-like proteins, frequenins, guanylate cyclase-activating proteins (GCAPs) and K^+-channel interacting proteins (KChiPs). NCS proteins are highly homologous and the three-dimensional structures of some prototypical NCS proteins show that they consist of two domains with two EF-hand-type Ca^{2+}-binding motifs each [5-7].

A distinctive feature of NCS proteins is that in spite of high degree of homology and structural similarity each Ca^{2+}-sensor can selectively regulate an intracellular target by sensing a specific narrow range of Ca^{2+} [5-7]. A fundamental question with respect to these observations is which structural elements account for the unique Ca^{2+}-sensitive target recognition events. Visual inspection of the primary structural alignment of NCS proteins reveals hypervariable amino acid sequence segments in the C-terminus of NCS proteins that are located after the fourth EF-hand.

Recoverin is a small neuronal calcium sensor protein that is involved in Ca^{2+}-dependent feedback mechanisms of photoreceptor cells by regulating rhodopsin kinase (RK) activity. RK and recoverin form a ternary complex with rhodopsin thereby preventing rhodopsin phosphorylation [9, 10]. A first structural analysis of the binary RK/recoverin complex has revealed that the N-terminus of RK forms an amphipathic α-helix, which interacts with a hydrophobic groove on the exposed surface of recoverin [10, 11]. The C-terminal region of recoverin (residues 190-202) was not resolved in this complex and therefore was out of scope of the intermolecular contacts revealed in this study. In previous biochemical and x-ray crystallo-graphic studies we have already demonstrated that the C-terminal segment in recoverin is an internal modulator of Ca^{2+}-sensitivity controlling the Ca^{2+}-myristoyl switch mechanism of recoverin and therefore the Ca^{2+}-dependence of recoverin binding to membranes and the range of Ca^{2+}-concentrations for recoverin regulation of rhodopsin kinase activity [8]. Investigation of recoverin C-terminus involvement in direct binding to RK was not undertaken so far.

In the present study we address the question, whether the C-terminus of recoverin could directly participate in interaction with RK and if so, what is the functional impact of this interaction on the physiological role of recoverin as inhibitor of RK.

EXPERIMENTAL PROCEDURES

Materials - $^{45}CaCl_2$ was purchased from Perkin Elmer (Germany) and [γ-^{32}P]ATP was from Hartmann Analytic GmbH Deutschland. CM5 Biacore sensor chips, Biacore coupling reagents, Glutathion-S-transferase (GST), goat anti-GST-antibody and CNBr-activated sepharose were from GE Healthcare. All other reagents were obtained from Sigma, Merck, Fluka, Serva and were at least analytical grade.

Cloning, heterologous expression and purification of recoverin forms - The truncated mutants of recoverin denoted Rc^{2-196}, Rc^{2-192}, Rc^{2-190}, Rc^{2-188}, Rc^{2-187}, Rc^{2-186}, Rc^{2-184} and point mutants denoted Rc^{P190G}, Rc^{Q191A}, Rc^{K192A} and Rc^{V193G} were obtained from a full-length recoverin cDNA in a pET-11d plasmid using standard site-directed mutagenesis procedures. For the production of each mutant DNA, a pair of oligonucleotide primers was employed in a polymerase chain reaction (PCR). Primers containing the bacteriophage T7 promotor sequence were used in the forward direction and a primer containing a stop codon and BamHI restriction site instead of the codon of the target amino acid was used in the reverse direction. The PCR fragments were inserted in a pET-11d plasmid between the NcoI and BamHI restriction sites. The screening for the mutant clones was performed using BglII restriction analysis. The integrity of the insert was confirmed by sequencing using the Sanger method. Heterologous expression of myristoylated recoverin forms in E.coli BL-21 (DE3) cells and their purification from cell lysates were performed as previously described [12]. The degree of myristoylation was determined by analytical high performance liquid chromatography using a reversed phase column (Phenomenex Luna 5µ C18, 4.6×250 mm) and was in most cases more than 95%. Concentrations of purified recoverin were determined using ε_{280} = 27,500 $M^{-1}cm^{-1}$ [13].

RK constructs and native RK - The N-terminal domain of RK corresponded to amino acids M1-G183, contained a glutathione-S-transferase (GST)-fusion part at the N-terminus and was denoted N-RK. Cloning, heterologous expression and purification of this construct was done according to a previously published procedure [9]. The single point mutant N-RK^{F3A} was created by standard cloning techniques. Native RK was purified from bovine rod outer segment (ROS) preparations as described earlier [14].

Fluorescence measurements - To determine the thermal stability of recoverin mutants, tryptophan fluorescence spectra at different temperatures were recorded using a Cary Eclipse spectrofluorimeter (Varian Inc.), equipped with a Peltier-controlled cell holder. Samples were measured in 20 mM Tris-HCl buffer (pH 8.0) containing 100 mM NaCl, 1 mM DTT and either 1 mM $CaCl_2$, or 1mM EDTA; protein concentration in samples was 10-15 µM. Recording of spectra and evaluation of data was as described [8, 15].

$^{45}Ca^{2+}$ binding assay and equilibrium centrifugation assay - Binding of $^{45}Ca^{2+}$ to wild-type recoverin and mutants and binding of recoverin mutants to ROS membranes using an equilibrium centrifugation assay was investigated as described previously [12, 16].

Phenyl-sepharose binding assay - The phenyl-sepharose binding assay was performed according to a published procedure [17]. Briefly, 2 µM wild-type recoverin or mutants were mixed with 100 µl phenyl-sepharose (GE Healthcare) and incubated at 37°C (Eppendorf thermomixer, 1,000 rpm) for 15 min in 20 mM HEPES, pH 7.5, 150 mM NaCl, 20 mM $MgCl_2$, 1mM DTT, 3 mM EGTA or 2 mM $CaCl_2$ (total volume, 1000 µl). The mixture was centrifuged for 15 min (14,000 rpm, table-top centrifuge Eppendorf model 5415), and protein concentration in the supernatant was determined by a Bradford protein assay (Bio-Rad).

Pull down assay - Interaction of recoverin forms with N-RK was tested using analytical affinity chromatography (pull down assay). Ten µg (in 50 µl) of the N-RK fragment carrying a GST tag was immobilized on glutathione sepharose by incubating it for 1 hour at 4°C (Eppendorf thermomixer, 1200 rpm) with 30 µl of 75% (v/v) suspension of glutathione sepharose in 20 mM Tris-HCl buffer (pH 7.5). Coupled to sepharose N-RK was washed two times with 1 ml of a buffer containing 20 mM Tris-HCl, pH 7.5, 100 mM NaCl, 1 mM DTT, 0.05% (v/v) Tween20 and 2 mM $CaCl_2$ or 5 mM EGTA to remove any non-bound protein. Last supernatant was removed and 10 µg of the corresponding recoverin form was applied to washed beads. The suspension was incubated for 1 hour at +4°C in the above-mentioned buffer in a total volume of 80 µl. After washing three times with 1 ml of the same buffer, the beads were treated with 30 µl of SDS sample buffer and eluted proteins were analyzed by Western blotting using an anti-recoverin antibody [18].

Surface plasmon resonance - Surface plasmon resonance (SPR) measurements were performed on a Biacore 2000 (GE Healthcare). Application of SPR technology in our laboratory and the analysis of data have been described in detail [19-21]. Specific adjustments of the procedure for the analysis of N-RK constructs are published in a recent report [9].

RK assay - The assay mixture in a final volume of 50 µl contained 10 µM rhodopsin (urea-washed ROS), 20 mM Tris-HCl, pH 7.5, 3 mM $MgCl_2$,1 mM [γ-^{32}P]ATP (30–100 dpm/pmol), 1mM EGTA, 1.26 mM $CaCl_2$, 1 mM DTT, 1 mM PMSF, 0.3 unit of RK and different concentrations of recoverin forms. The reaction was initiated by the addition of ATP, and samples were incubated in continuous light for 30 min at 37°C. Incubation was terminated by adding 1 ml of 10% (w/v) trichloroacetic acid. The resulting precipitate was collected by centrifugation and washed 3-4 times with 1 ml of 10% trichloroacetic acid; the pellet was used for Cerenkov counting.

Modeling the N-RK$^{1-25}$/recoverin complex and docking simulations - The crystallographic structure available at highest resolution (1.50 Å) of non-myristoylated wild-type bovine recoverin (PDB entry: 1OMR) was used as a template for the recoverin C-terminus [14]. The region corresponding to the amino acid stretch E181-Q187 was superposed to the average NMR structure of the N-RK$^{1-25}$/recoverin complex [10] (PDB entry: 2I94; in such complex only residues 1-16 of the N-RK peptide were resolved; recoverin residues 190-201 are missing), in which duplicate atoms, water molecules and hydrogens were removed. The superposition led to a Cα-RMSD of 2.4 Å. The 2I94 complex structure was truncated at I186, and the

strand corresponding to recoverin C-terminus (Q187-L202) was merged from the superposed 1OMR structure. Polar hydrogens were then added and the complex was energy-minimized in vacuum by 1500 steps of steepest descent with an average gradient tolerance of 0.001 kcal/mol. This procedure led to the Rc^{8-202}/N-RK^{1-16} complex used as native in further computations (shown in Figures 4A and 7).
Truncated forms of native recoverin were prepared *in silico* (Table 2) in line with experimental variants, and three sets of rigid-body docking simulations between each recoverin variant (target) and the N-RK^{1-16} peptide (probe) with randomized initial positions were performed by using a well established protocol [22, 23], thus generating for each docked complex 12,000 different solutions, i.e. corresponding to relative target/probe coordinates. Each *i*-docking solution is characterized by a score index (ZD*i*) that quantifies shape complementarity, electrostatics and desolvation of the interface upon binding of each docked complex [24], and is ranked accordingly (i.e. 1 = best scored solution; 12,000 = worst scored solution). For each docking simulation, the native-like solutions ZDi^N, which structurally resemble that of the native modeled complex (Cα-RMSD <1 Å), were then clustered and analyzed as described before [25] and an average docking score (ZD-s) was calculated for each cluster starting from the score of each individual native-like complex (Table 2):

$ZD-s=\frac{\sum_i ZD_i^N}{M}$, in which the cluster groups *M* native-like solutions. Such ZD-s index is a convenient empirical descriptor of the affinity in protein-protein interactions occurring without major structural rearrangements as it is linearly correlated with ΔG [22]. Therefore we employed it to predict the effect of Rec truncations on its affinity for the N-RK peptide.

RESULTS

NCS proteins exhibit high amino acid homology in the core part of their structure that mainly encompasses the EF-hand domains. A general feature of the NCS proteins structure is a number of conservative hydrophobic residues (Fig. 1A, highlighted in bold) localized in the N-terminal lobe and implicated in target binding [26-28]. Differences in the amino acid sequences of NCS proteins are most prominent at the N- and C-terminal parts (Fig. 1 A). Based on our previous findings that the C-terminus of recoverin operates as an internal modulator of Ca^{2+}-sensitivity and contributes significantly to the thermal stability of the protein [8] we set out to determine the critical amino acids and amino acid length of the C-terminus with respect to these properties. By this approach we also found that the C-terminus participates in the interaction with RK.

We prepared several mutants of recoverin with different length of the C-terminal region (Fig. 1B, upper part). The amino acid sequence of the shortest form Rc^{2-184} ended after 4th EF-hand of the protein. Truncated recoverin forms were purified from *E.coli* extracts after heterologous expression by a standard protocol to apparent homogeneity. They showed a decreased electrophoretic mobility consistent with their reduced molecular mass (Fig. 1B, lower part). All recoverin forms were expressed with an attached myristoyl group as previously described for WT recoverin and other mutants. The extent of myristoylation of every recoverin mutant used in this study was determined by reversed phase HPLC yielding a degree of myristoylation exceeding 95 % for the mutants $Rc^{2–196}$, $Rc^{2–192}$, $Rc^{2–190}$, $Rc^{2–188}$, while shorter constructs had a reduced level of myristoylation (60-80%) indicating an altered conformation.

Thermal stability of recoverin mutants – Thermal unfolding of recoverin can be monitored by heat-induced changes in the maximum position of the fluorescence spectrum of its tryptophanyls (Fig. 2). In general, the Ca^{2+}-free (apo) recoverin was less thermostable than the Ca^{2+}-bound form by 12-16 °C (Table 1). Down to a length of 188 amino acids the truncation did not affect the thermal stability, remaining nearly constant without regard to Ca^{2+} content (Fig. 2C). Further shortening of the C-terminus, however, led to decreased thermal stability. For example, apo-Rc^{2-186} exhibits a decrease in mid-transition temperature for 7-9 °C (Fig. 2B and Table 1). The notable decrease in thermal stability and myristoylation level of recoverin mutants below a protein length of 188 amino acids demonstrate essential structural disturbance in the protein. Therefore the respective recoverin mutants were excluded from the further analysis.

$^{45}Ca^{2+}$ and ROS membrane-binding – A step-wise truncation of the C-terminus can impair the affinity of recoverin for Ca^{2+}. Direct binding of Ca^{2+} was measured using the $^{45}Ca^{2+}$-binding assay and yielded the

higher K_D-values the more amino acids were cut (Table 1). Whereas Rc^{2-196} was similar to the WT, Rc^{2-188} exhibited two-fold lower affinity. Similarly to WT recoverin the binding of Ca^{2+} to these mutants was cooperative as indicated by Hill coefficients between 1.55 and 1.9. The change in the affinity for Ca^{2+} in truncated recoverin mutants suggested alterations in the Ca^{2+}-myristoyl switch mechanism of the protein underlying its binding to membranes. One may expect a shift in Ca^{2+}-dependence of the binding to a higher free Ca^{2+} concentration. Indeed, as revealed from analysis of the binding of truncated recoverin forms to native washed ROS membranes, the value of half-maximal free calcium concentration for binding to membranes of Rc^{2-196} was similar to that of WT while Rc^{2-188} exhibited a 1.5-fold shift to higher free calcium concentration (Table 1). Together these results showed that the C-terminus is important for regulating the Ca^{2+}-sensitivity of recoverin thereby confirming previous conclusion on the mutant Rc^{2-190} [8]. Importantly, the changes in Ca^{2+}-sensitivity were not related to any mutation-induced protein stability changes, which are absent in our case (Fig. 2 and Table 1).

Interaction with RK – The N-terminal part of RK forms an amphipathic helix that interacts with an exposed hydrophobic groove in recoverin [10, 11]. We tested interaction of truncated recoverin mutants with the N-terminal domain of rhodopsin kinase by a pull down assay and surface plasmon resonance spectroscopy (Fig. 3). GST-fusion constructs of the N-terminal domain of RK (N-RK) were immobilized on glutathione-sepharose and incubated with recoverin WT and mutants in the presence and absence of Ca^{2+}. The Ca^{2+}-concentration was saturating in all cases. All recoverin forms showed a Ca^{2+}-induced interaction with N-RK, but mutants with a truncated C-terminus bound less strongly to N-RK, especially Rc^{2-190} and Rc^{2-188} (Fig. 3A). We confirmed this result by immobilizing N-RK on a sensor chip surface and flushing 14 µM recoverin WT and mutants over the N-RK coated surface. Positive amplitudes indicated binding of recoverin to N-RK and gave a first hint about relative binding affinities. Mutants showed lower binding amplitudes than WT (Fig. 3B), which is in agreement with the decreased intensity of the protein bands shown in Fig. 3A. For further quantifying these results we performed titration series with all recoverin mutants on N-RK-coated sensor chips. Recoverin forms were injected into the flow system at concentrations between 0.1 and 220 µM (Fig. 3C). Apparent affinity constants (K_D in Table 1) correspond to the concentration at which the response amplitudes were half maximal. The difference in the apparent K_D for WT and Rc^{2-188} was 7.8-fold; the mutants Rc^{2-196}, Rc^{2-192}, Rc^{2-190} differed by factors of 3.4, 4.1 and 6.8, respectively (Table 1). We next asked, whether the decrease in binding affinity might have a functional consequence in regulating RK activity. At saturating Ca^{2+}-concentration WT recoverin prevented RK from phosphorylating rhodopsin by forming a ternary complex. Kinase activity was less inhibited by truncated mutants (Fig. 3D). For example, the inhibitory response curve with Rc^{2-188} was shifted to higher concentrations of recoverin. A comparison of all tested mutants at a fixed recoverin concentration (14 µM) revealed an almost gradual decrease in inhibitory efficiency, when the C-terminus was more and more cut off (Fig. 3D, inset). The shift in the inhibitory response curve is consistent with a lower affinity of the mutants for RK (Fig. 3 C and D). The lower affinity, however, did not result from a changed or disturbed exposition of hydrophobic regions in recoverin, since the mutants showed the same Ca^{2+}-dependent binding to phenyl-sepharose as WT recoverin (data not shown). In summary we conclude from our data that the C-terminus of recoverin participates not only in regulating its Ca^{2+}-sensitivity, but that it is also involved in direct interaction with RK and thereby controls the inhibitory effect of recoverin.

Modeling of the recoverin/N-RK protein complex structure – To investigate whether an involvement of the C-terminus of recoverin in the interaction with the N-terminal region of RK is feasible from a structural point of view we built a model of the recoverin/N-RK complex focusing on the interaction interface involving the C-terminus of recoverin. The available three-dimensional NMR-structure of recoverin in complex with the N-terminal fragment of rhodopsin kinase ($N\text{-}RK^{1-25}$) was used as a template [10]. Further, the missing C-terminal fragment of the recoverin NMR-structure was taken from the crystallographic structure of nonmyristoylated recoverin having this element resolved [14]. The obtained model of the complex revealed a position of recoverin´s C-terminal α-helix (highlighted in red, Fig. 4A) in close proximity to the N-terminal kinase peptide (highlighted in blue, Fig. 4A). While the main part of the N-RK peptide is deeply buried inside a hydrophobic groove of recoverin, the first amino acids of N-RK helix form a contact interface with the C-terminal region of recoverin (Fig. 4A).

The resulting model was used to perform rigid body docking simulations of the interaction process of N-RK with the truncated recoverin forms that we employed in pull-down and SPR experiments. Applied

docking simulations suggested significantly different roles for the various portions of recoverin´s C-terminus in modulating RK recognition. While the relative population of native-like solutions was the highest for WT recoverin (5.4%; see Table 2), it remained constant to ~5.0 % for all the subsequent truncations up to the shortest stretch (Rc^{8-188}), for which it reduced to 3.4 %. The best-scored solutions, in line, were found to be native-like in each independent docking run up to the Rc^{8-190} form, and they were ranked even lower for the Rc^{8-188} variant. Both the statistics and the average scores of the ensembles of reconstituted complexes (Table 2) are significantly affected by the truncation, especially for the 8-190 and 8-188 variants, hence suggesting a major role of the 189-192 residues.

A highly significant correlation (R= 0.97) was found between the average scores of ensembles of reconstituted complexes (ZD-s) and the experimental affinity measured by SPR (Figure 4B; for clarity we plot the K_D instead of the lnK_D on the x-axis). The ZD-s index is known to linearly correlate with the free-energy of binding of protein-protein complexes that form in water soluble and in membrane environments without major conformational changes in either protein [22, 23, 25, 29, 30]. Hence, such correlation corroborates the reliability of the three-dimensional model of the complex and suggests that the effect of truncation is not to perturb the remaining structure of recoverin, which appears to be stable independent of the truncated portion, a hypothesis indirectly confirmed by our thermal denaturation studies. Moreover, such correlation further suggests that the binding with the N-RK peptide may occur in a rigid-body like manner.

Protein-protein interface of the recoverin/N-RK complex – The structural analysis of the model suggested that a stretch of residues included in the 190-193 sequence of recoverin C-terminus might interact directly with residues from the N-terminal amphipathic helix of RK, presumably with F3. We constructed the corresponding point mutants, expressed them heterologously in *E.coli* and purified them to apparent homogeneity (Fig. 5). The recoverin point mutations did not affect the thermal stability of the protein, neither in the apo- nor in the Ca^{2+}-bound form (Table 3). $^{45}Ca^{2+}$-binding was only slightly different for the Rc^{P190G} mutant (K_D was 25.1 µM in comparison to 19.2 µM for WT) and the cooperativity was lower for the Rc^{Q191A} mutant. All recoverin point mutants bound to membranes in the presence of Ca^{2+} similar to WT with EC_{50} values that were centered on 4.5 µM. Thus neither Ca^{2+}-binding properties nor Ca^{2+}-dependent membrane association of recoverin were affected by introduced mutations. Interaction of recoverin point mutants with N-RK was studied in the same manner as the interaction with the truncated mutants (Fig. 3 and Fig. 6). All mutants with the exception of Rc^{Q191A} had a lower affinity for N-RK as it became visible by pull down experiments (Fig. 6A) and SPR measurements (Fig. 6B). However, the increase of the apparent K_D values was not so pronounced as what we observed with the truncated mutants (Table 3). The highest K_D of 34.1 µM was measured with the Rc^{K192A} mutant (Fig. 6B) indicating that K at this position is of critical importance for the interaction with RK. Point mutations also diminished the inhibitory effect of WT recoverin on RK and the effect was largest with the mutants Rc^{K192A} and Rc^{V193G} (Fig. 6C, inset), both also displayed the lowest apparent affinity for N-RK among all tested point mutants (Table 3). The mutant Rc^{Q191A} was slightly anomalous in this aspect as it had a reduced ability to inhibit RK, although its affinity to RK was like in WT recoverin.

We also tested the effect of substituting F at position 3 in N-RK. This residue is situated in close proximity to the C-terminal α-helix of recoverin in the model of the recoverin/N-RK complex and therefore might have a crucial role in the interaction process. We mutated this residue to A and examined effects of this substitution on the apparent affinity to recoverin. Employing SPR spectroscopy in series of recoverin titration experiments we observed that the binding amplitudes of WT recoverin interacting with $N\text{-}RK^{F3A}$ were sufficiently diminished (Fig. 6B). This is consistent with our suggestion that F at position 3 is of primary importance for the recoverin C-terminus interaction with N-RK. The effect was similar to the one we observed for the binding of N-RK to the mutant Rc^{2-188} having C-terminal α-helix completely deleted by truncation (Fig. 3C), which further supports crucial role of F3.

DISCUSSION

The turnoff of a photoreceptor light response depends critically on the timely phosphorylation of rhodopsin by RK [31]. This step is under Ca^{2+}-dependent control of the NCS protein recoverin operating in a ternary complex [9, 10]. Since the Ca^{2+}-dependent regulation of RK activity is of critical importance

for the sensitivity regulation of a photoreceptor cell [32] we focused in the present work on the structural basis of this regulatory step. The C-terminus of recoverin was described in a previous publication as an internal modulator of Ca^{2+}-sensitivity [8]. We here extend this work by showing that the C-terminus of recoverin (F188-L202) not only influences the binding of Ca^{2+}, but is also critical for the affinity of recoverin binding to RK (for summary of these data see Table 1). By this approach we discovered a novel interaction site at the recoverin/RK protein-protein interface.

Since our conclusions are based on experiments employing truncated recoverin forms it is important to verify that the decrease in affinity for Ca^{2+} and N-RK was not caused by defective folding of recoverin mutants. Using thermal denaturation studies we showed that mutants $Rc^{2\text{-}196}$, $Rc^{2\text{-}192}$, $Rc^{2\text{-}190}$ and $Rc^{2–188}$ have the same structural stability as recoverin WT and in the same time they exhibited lower affinity towards N-RK binding (Table 1 and Fig. 2A). However further shortening of recoverin C-terminus in mutants $Rc^{2–187}$, $Rc^{2–186}$ and $Rc^{2–184}$ revealed progressive destabilization of the recoverin tertiary structure. In our previous publication [8], we indicated critical residues F188 and I186 forming a link to the cluster of non-polar residues in the central part of recoverin structure (EF-hands 3 and 4). These contacts contribute to the hydrophobic core of recoverin and disturbing them in the mutants $Rc^{2–187}$, $Rc^{2–186}$ and $Rc^{2–184}$ destabilized the protein structure. Of lesser importance for these intramolecular interactions are residues following F188 at the C-terminus. However the data presented in this study indicate their important role for intermolecular interaction of recoverin with RK.

The Ca^{2+}-induced conformational change in recoverin exposes a number of non-polar amino acids in the N-terminal region that are involved in the interaction of recoverin to RK and a recent NMR study using a 25 amino acid peptide of the N-terminus of RK ($RK^{1\text{-}25}$) revealed that the RK peptide adopts an amphipathic helix fitting into the hydrophobic groove of recoverin [10, 11]. Other members of the NCS protein family like KChIP1 [26], GCAP2 [27] and yeast frequenin [33] harbor also hydrophobic grooves considered to be important for target interaction. Previous studies have also shown an involvement of C-terminal part of NCS proteins in their binding to target [26, 34-37]. Using surface plasmon resonance measurements and pull-down assays we found that the same is true for the C-terminus of recoverin. Importantly, the revealed effects of reduced affinity of recoverin C-terminal mutants to RK are not the result of an alteration in the Ca^{2+}-sensitivity of recoverin, since all the experiments were done at saturating Ca^{2+} concentrations when recoverin is already in the Ca^{2+}-loaded state. Moreover, the studied recoverin point mutants have almost the same Ca^{2+}-sensitivity as WT recoverin but lower affinity to RK (Table 3).

The C-terminal α-helix of recoverin following the kink caused by P190 provides additional contacts to the RK peptide, as it is apparent from the visual inspection of the three-dimensional model of recoverin/N-RK complex (Fig. 4A). Further, our modeling approach highlighted the possible involvement of four amino acids in the C-terminus (P190-V193) (Fig. 4A). Thus, the N-terminal peptide of RK is retained in the complex not only by hydrophobic groove of recoverin, but additional contacts within the C-terminus of recoverin provide more tight interaction and proper positioning of the target peptide. Our rigid body docking simulations revealed sufficient decrease of kinase peptide binding energy upon step-wise truncation of recoverin C-terminal α-helix, which is in agreement with the K_D values on interaction of truncated recoverin forms to immobilized N-RK (Table 1 and Fig. 4B).

The major effect observed experimentally with the point mutant Rc^{K192A} (3.2-fold lower affinity for N-RK, Table 3 and 8.6-fold less inhibitory efficiency, Fig. 6C) was also in the agreement with structural analysis. K192 was predicted to form a cation-π interaction pair with the aromatic ring of F3 in N-RK following the minor rearrangement of both residues side groups for optimal contact (Fig. 7). Figure 7 also highlights a salt bridge between K192 and E188 at recoverin C-terminus. Such electrostatic interaction is expected to stabilize the orientation of the subsequent α-helix, hence providing an optimal orientation of the whole helix and creating the conditions for tight binding of F3 through cation-π interaction with K192. We confirmed these structural interpretations by measuring the affinity of the corresponding point mutant $N\text{-}RK^{F3A}$ for recoverin that resulted in a similar affinity like we obtained for the truncated recoverin mutant $Rc^{2\text{-}188}$ and N-RK (Fig. 6B). These results were also broadly consistent with recent work using several point mutants of a 15 amino acid peptide of N-RK [11]. For example, mutations at positions F3 and L6 cause a complete loss of recoverin binding in pull-down assays. While the residue L6 forms the tight contact with residues of the hydrophobic groove in recoverin [10], the interaction partner for residue F3 until the start of the current study was unknown.

Site-specific mutations of the three other amino acid residues in recoverin C-terminus (P190G, Q191A and V193G) revealed a two- to three-fold lower N-RK affinity for Rc^{P190G} and Rc^{V193G}, but no effect of mutation at Q191. Since P is known to determine the direction of an α-helix when located at the beginning of it, it probably helps to maintain the correct orientation of recoverin C-terminus to the N-RK residues. A mutation to G would allow more flexibility and thus a less optimal interface. V193 is faced almost at the opposite site of the helix with respect to the RK peptide and therefore is very likely not located in the interface region. G is known as helix breaker and its placement in position 193 instead of V could therefore perturb the secondary structure of the whole C-terminal α-helix, thereby decreasing the protein affinity to N-RK (Table 3).

Taking together, our results demonstrate an important role of C-terminal segment of recoverin for RK targeting. We found that the binding surface for RK is not limited by the hydrophobic groove within N-terminal lobe of recoverin but also includes the last α-helix of C-terminal lobe. Involvement of distinct regions including the C-terminus in target binding or recognition is not uncommon among NCS proteins as this has been described for KChIP1 [26] and GCAP1 [34-37]. It will be of interest to see, whether the cation-π interactions that have been observed in ligand-receptor interactions as well as in enzymatic catalysis [38] contribute also significantly to NCS protein related target recognition.

ACKNOWLEDGEMENTS

We thank Dmitry V. Zinchenko for the HPLC analysis of recoverin samples.

FUNDING

This work was supported by grants from Russian Foundation for Basic Research to I.I.S. (09-04-01778-a) and to E.Yu.Z. (09-04-00666-a), a grant from the President of Russia (MD-4423.2010.4) to I.I.S, in part by a grant to P.P.Ph. from the Russian Foundation for Basic Research (# 09-04-00395) and a grant from the Program of the Russian Academy of Sciences "Molecular and Cellular Biology" to P.E.A. It was also supported by grants from the Deutsche Forschungsgemeinschaft (DFG) to K.W.K. (KO948/7-1; KO948/7-2). The use of the computer cluster for simulations was supported by the EC integrated Project DIRAC, in the 6th FWP under IST-02778. D.D.O. is the recipient of an Alexander von Humboldt Fellowship.

REFERENCES

1 Berridge, M. J., Lipp, P. and Bootman, M. D. (2000) The versatility and universality of calcium signalling. Nat. Rev. Mol. Cell. Biol. **1**, 11-21
2 Ikura, M. and Ames, J. B. (2006) Genetic polymorphism and protein conformational plasticity in the calmodulin superfamily: two ways to promote multifunctionality. Proc. Natl. Acad. Sci. USA **103**, 1159-1164
3 Rizo, J., and Sudhof, T. C. (1998) C2-domains, structure and function of a universal Ca2+-binding domain. J. Biol. Chem. **273**, 15879-15882
4 Lewit-Bentley, A., and Rety, S. (2000) EF-hand calcium-binding proteins. Curr. Opin. Struct. Biol. **10**, 637-643
5 Burgoyne, R. D. (2007) Neuronal calcium sensor proteins: generating diversity in neuronal Ca2+ signalling. Nat. Rev. Neurosci. **8**, 182-193
6 Philippov, P. P. and Koch, K.-W. (eds). (2006) Neuronal Calcium Sensor Proteins. Nova Publishers, Hauppauge, NY
7 Burgoyne, R. D. and Weiss, J. L. (2001) The neuronal calcium sensor family of Ca2+-binding proteins. Biochem. J. **353**, 1-12
8 Weiergräber, O. H., Senin, II, Zernii, E. Y., Churumova, V. A., Kovaleva, N. A., Nazipova, A. A., Permyakov, S. E., Permyakov, E. A., Philippov, P. P., Granzin, J. and Koch, K. W. (2006) Tuning of a neuronal calcium sensor. J. Biol. Chem. **281**, 37594-37602
9 Komolov, K. E., Senin, II, Kovaleva, N. A., Christoph, M. P., Churumova, V. A., Grigoriev, II, Akhtar, M., Philippov, P. P. and Koch, K. W. (2009) Mechanism of rhodopsin kinase regulation by recoverin. J. Neurochem. **110**, 72-79

10 Ames, J. B., Levay, K., Wingard, J. N., Lusin, J. D. and Slepak, V. Z. (2006) Structural basis for calcium-induced inhibition of rhodopsin kinase by recoverin. J. Biol. Chem. **281**, 37237-37245
11 Higgins, M. K., Oprian, D. D. and Schertler, G. F. (2006) Recoverin binds exclusively to an amphipathic peptide at the N terminus of rhodopsin kinase, inhibiting rhodopsin phosphorylation without affecting catalytic activity of the kinase. J. Biol. Chem. **281**, 19426-19432
12 Senin, II, Fischer, T., Komolov, K. E., Zinchenko, D. V., Philippov, P. P. and Koch, K. W. (2002) Ca2+-myristoyl switch in the neuronal calcium sensor recoverin requires different functions of Ca2+-binding sites. J. Biol. Chem. **277**, 50365-50372
13 Johnson, W. C., Jr., Palczewski, K., Gorczyca, W. A., Riazance-Lawrence, J. H., Witkowska, D., and Polans A. S. (1997) Calcium binding to recoverin: implications for secondary structure and membrane association. Biochim. Biophys. Acta **1342**, 164-174
14 Weiergraber, O. H., Senin, II, Philippov, P. P., Granzin, J. and Koch, K. W. (2003) Impact of N-terminal myristoylation on the Ca2+-dependent conformational transition in recoverin. J. Biol. Chem. **278**, 22972-22979
15 Permyakov, S. E., Khokhlova, T. I., Uversky, V. N. and Permyakov, E. A. (2010) Analysis of Ca2+/Mg2+ selectivity in alpha-lactalbumin and Ca(2+)-binding lysozyme reveals a distinct Mg(2+)-specific site in lysozyme. Proteins **78**, 2609-2624
16 Zozulya, S. and Stryer, L. Calcium-myristoyl protein switch. (1992) Proc. Natl. Acad. Sci. USA **89**, 11569-11573
17 Komolov, K. E., Zinchenko, D. V., Churumova, V. A., Vaganova, S. A., Weiergraber, O. H., Senin, II, Philippov, P. P. and Koch, K. W. (2005) One of the Ca2+ binding sites of recoverin exclusively controls interaction with rhodopsin kinase. Biol. Chem. **386**, 285-289
18 Lambrecht, H. G. and Koch, K. W. (1992) Recoverin, a novel calcium-binding protein from vertebrate photoreceptors. Biochim. Biophys. Acta **1160**, 63-66
19 Lange, C. and Koch, K. W. (1997) Calcium-dependent binding of recoverin to membranes monitored by surface plasmon resonance spectroscopy in real time. Biochemistry **36**, 12019-12026
20 Koch, K. W. (2000) Identification and characterization of calmodulin binding sites in cGMP-gated channel using surface plasmon resonance spectroscopy.Methods Enzymol. **315**, 785-797
21 Komolov, K. E., Senin, II, Philippov, P. P. and Koch, K. W. (2006) Surface plasmon resonance study of g protein/receptor coupling in a lipid bilayer-free system. Anal. Chem. **78**, 1228-1234
22 Dell'Orco, D. (2009) Fast predictions of thermodynamics and kinetics of protein-protein recognition from structures: from molecular design to systems biology. Mol. Biosyst. **5**, 323-334
23 Dell'Orco, D., Seeber, M., De Benedetti, P. G. and Fanelli, F. (2005) Probing fragment complementation by rigid-body docking: in silico reconstitution of calbindin D9k. J. Chem. Inf. Model **45**, 1429-1438
24 Chen, R. and Weng, Z. (2003) A novel shape complementarity scoring function for protein-protein docking. Proteins **51**, 397-408
25 Dell'Orco, D., De Benedetti, P. G. and Fanelli, F. (2007) In silico screening of mutational effects on enzyme-proteic inhibitor affinity: a docking-based approach. BMC Struct. Biol. **7**, 37
26 Zhou, W., Qian, Y., Kunjilwar, K., Pfaffinger, P. J. and Choe, S. (2004) Structural insights into the functional interaction of KChIP1 with Shal-type K(+) channels. Neuron **41**, 573-586
27 Ermilov, A. N., Olshevskaya, E. V. and Dizhoor, A. M. (2001) Instead of binding calcium, one of the EF-hand structures in guanylyl cyclase activating protein-2 is required for targeting photoreceptor guanylyl cyclase. J. Biol. Chem. **276**, 48143-48148
28 Tachibanaki, S., Nanda, K., Sasaki, K., Ozaki, K. and Kawamura, S. (2000) Amino acid residues of S-modulin responsible for interaction with rhodopsin kinase. J. Biol. Chem. **275**, 3313-3319
29 Dell'Orco, D., Casciari, D. and Fanelli, F. (2008) Quaternary structure predictions and estimation of mutational effects on the free energy of dimerization of the OMPLA protein. J. Struct. Biol. **163**, 155-162
30 Dell'Orco, D., De Benedetti, P. G. and Fanelli, F. (2007) In silico screening of mutational effects on transmembrane helix dimerization: insights from rigid-body docking and molecular dynamics simulations. J. Phys. Chem. B **111**, 9114-9124
31 Mendez, A., Burns, M. E., Roca, A., Lem, J., Wu, L. W., Simon, M. I., Baylor, D. A. and Chen, J. (2000) Rapid and reproducible deactivation of rhodopsin requires multiple phosphorylation sites. Neuron **28**, 153-164

32 Chen, C.-K., Woodruff, M. L., Chen, F. S., Chen, D. and Fain, G. F. (2010) Background light produces a recoverin-dependent modulation of activated-rhodopsin lifetime in mouse rods. J. Neurosci. **30**, 1213-1220
33 Strahl, T., Huttner, I. G., Lusin, J. D., Osawa, M., King, D., Thorner, J. and Ames, J. B. Structural insights into activation of phosphatidylinositol 4-kinase (Pik1) by yeast frequenin (Frq1). (2007) J. Biol. Chem. **282**, 30949-30959
34 Krylov, D. M., Niemi, G. A., Dizhoor, A. M. and Hurley, J. B. (1999) Mapping sites in guanylyl cyclase activating protein-1 required for regulation of photoreceptor membrane guanylyl cyclases. J. Biol. Chem. **274**, 10833-10839
35 Schrem, A., Lange, C., Beyermann, M. and Koch, K. W. (1999) Identification of a domain in guanylyl cyclase-activating protein 1 that interacts with a complex of guanylyl cyclase and tubulin in photoreceptors. J. Biol. Chem. **274**, 6244-6249
36 Li, N., Sokal, I., Bronson, J. D., Palczewski, K. and Baehr, W. (2001) Identification of functional regions of guanylate cyclase-activating protein 1 (GCAP1) using GCAP1/GCIP chimeras. Biol. Chem. **382**, 1179-1188
37 Hwang, J. Y., Schlesinger, R. and Koch, K. W. (2004) Irregular dimerization of guanylate cyclase-activating protein 1 mutants causes loss of target activation. Eur. J. Biochem. 271, 3785-3793
38 Zacharias, N. and Dougherty, D. A. (2002) Cation-pi interactions in ligand recognition and catalysis. Trends Pharmacol. Sci. **23**, 281-287

FIGURE LEGENDS

Figure 1: (A) Multiple sequence alignment of NCS proteins. The sequences of bovine GCAP1, recoverin and neurocalcin and from human frequenin and KChIP1 are shown. Secondary structural elements (α-helices and β-sheets) are indicated and the functional Ca^{2+}-binding regions EF-hand 2 and EF-hand 3 are highlighted in gray. Amino acids of hydrophobic pocket are shown in bold and framed in gray. The residues outlined in box correspond to the "C-terminal segment". **(B)** SDS-PAGE analysis of purified C-terminal truncated forms of recoverin. C-terminal sequences of mutant forms in comparison to wild-type are shown above the gel.

Figure 2: Thermal stability of C-terminal truncated recoverin forms according to the data of tryptophan fluorescence of the protein. The maximum position of fluorescence spectrum (λ_{max}) was recorded at increasing temperature in the presence of 1 mM $CaCl_2$ (filled symbols) or 1 mM EDTA (open symbols). **(A)** Thermal unfolding of truncated recoverin forms (Rc^{2-196} to Rc^{2-188}) that exhibited WT-like thermal stability. **(B)** Thermal unfolding of Rc^{2-186}, exhibiting decreased thermal stability. A similar behavior was observed for mutants Rc^{2-187} and Rc^{2-184} (not shown). **(C)** Mid-transition temperatures ($T_{1/2}$) for thermal unfolding of Ca^{2+}-loaded (squares) and apo-forms (circles) of truncated recoverin mutants. The $T_{1/2}$ values are plotted against protein length of recoverin. The mutants with destabilized structure are separated from the mutants with WT-like stability by a vertical dashed line.

Figure 3: Effect of recoverin C-terminal truncation on its binding to N-RK. **(A)** Pull-down assay demonstrating dependence of recoverin binding to N-RK on the length of recoverin C-terminus. All recoverin forms containing a truncated C-terminus showed a lower binding to N-RK than WT. The N-terminal domain of RK was immobilized on glutathione-sepharose and used to pellet apo- or Ca^{2+}-loaded forms of recoverin. Bound proteins were eluted from the sorbent by SDS-PAGE sample-buffer and analysed by SDS-PAGE and Western-blotting. Recoverin content in each case was detected by anti-recoverin antibodies. **(B)** A representative overlay of SPR sensorgrams showing real-time binding of C-terminal truncated recoverin mutants to N-RK. N-RK was anchored on the sensor-chip surface via its GST tag using anti-GST antibodies covalently coupled to the dextran matrix. Ca^{2+}-loaded forms of recoverin were injected over the N-RK surface to obtain binding curves. Concentration of recoverin during runs in each case was 14 μM. The reference signal from a control surface with immobilized GST was subtracted. **(C)** Steady-state affinity analysis of C-terminal truncated recoverin binding to N-RK by SPR spectroscopy. Binding of truncated recoverin forms was recorded at different concentrations of recoverin and the amplitudes of binding signals at equilibrium were determined, normalized and shown as function of recoverin concentration. Concentration of recoverin was varied from 0.1 to 220 μM. **(D)** Inhibition of rhodopsin kinase by WT and Rc^{2-188}. Rhodopsin kinase activity was measured by *in vitro* phosphorylation assay in the presence of 200 μM free Ca^{2+}. Concentration of WT and mutant Rc^{2-188} was

varied within 0-0.1 mM and 0-1.0 mM, respectively. Phosphorylation of rhodopsin in the presence of other truncated forms of recoverin is shown in the inset and was measured at 14 µM recoverin.

Figure 4: Modelling the recoverin-RK^{1-25} complex using rigid body docking. **(A)** Three-dimensional model of the recoverin-RK^{1-25} complex. The model is based on the available NMR structure of the recoverin-RK^{1-25} complex (PDB entry: 2I94, ref. 10) fused with the X-ray crystallographic structure of the C terminus of recoverin (PDB entry: 1OMR, ref 14). Only residues 1-16 in RK are shown, while the structure of recoverin comprehends residues 8-202 (See Methods). The RK^{1-25} peptide is shown in blue, while recoverin is shown in gray except its C-terminus that is shown in red. Calcium ions are represented by green spheres. On the left, a ribbon representation shows the secondary structure of the complex and the residues targeted by mutagenesis are labeled and shown in sticks. On the right, the molecular surface of the complex is shown from the same perspective. **(B)** Plot of average docking scores (ZD-s) of the clusters containing native-like solutions for each truncated recoverin forms versus experimental affinity data for the RK peptide. The linear regression fitting curve is shown (R = 0.97).

Figure 5: SDS-PAGE analysis of purified C-terminal point mutants of recoverin. C-terminal sequence of recoverin is shown above the gel with amino acid substitutions highlighted in bold.

Figure 6: Effect of single amino acid substitutions in the C-terminus of recoverin on its interaction to N-RK. **(A)** Pull-down assay with recoverin point mutants after binding to N-RK immobilized on glutathione-sepharose. The conditions were the same as applied for truncated mutants (Fig. 3A). Recoverin bound on N-RK was visualised by anti-recoverin antibodies. **(B)** Effect of single amino acid substitution in N-RK and in the C-terminus of recoverin on binding affinity measured by SPR spectroscopy. Binding of recoverin point mutants was recorded at different concentration of recoverin and SPR amplitudes at equilibrium were determined, normalized and shown as a function of recoverin concentration, which was varied from 0.1 to 175 µM. The same protocol was used for recordings with WT recoverin and the N-RK^{F3A} mutant, which resulted in an apparent K_D of 65.2 µM ± 6.7 µM (s.d.). **(C)** Inhibition of rhodopsin kinase by WT and Rc^{K192A}. RK activity was measured by *in vitro* phosphorylation assay in the presence of 200 µM free Ca^{2+}. Phosphorylation of rhodopsin in the presence of other point mutants of recoverin is shown in the inset and was measured at 38 µM recoverin.

Figure 7: Structural details of the N-RK/recoverin interaction highlighting the contact region involving the C-terminus of recoverin and RK^{1-25}. The residue suggested to be most important for the interaction are shown in sticks and labeled (blue F3 from RK and red K192 and E188 from recoverin).

Biochemical Journal Immediate Publication. Published on 08 Feb 2011 as manuscript BJ20110013

TABLE 1

The effect of recoverin C-terminal truncation on the thermal stability of the protein, its calcium binding parameters, Ca^{2+}-dependent interaction with ROS-membranes and the affinity for N-RK

Recoverin form	Thermal denaturation[a]		Binding of calcium[c]		Binding to membranes[d]		Affinity for N-RK[e]
	$T_{1/2}$, °C apo form	$T_{1/2}$, °C Ca^{2+}-bound form	K_D, μM	Hill coefficient	EC_{50}, $[Ca^{2+}]_f$ (μM)	Hill coefficient	K_D, μM
WT	65.1	79.8	19.2 ± 0.4	1.78	3.5 ± 0.2	2.0	10 ± 0.6
2-196	68.8	80.6	19.7 ± 0.6	1.73	3.3 ± 0.2	2.2	34 ± 1.7
2-192	65.8	78.6	26.2 ± 1.0	1.90	4.1 ± 0.3	1.75	41 ± 2.4
2-190	66	79.6	36.8 ± 3.5	1.55	5.9 ± 0.6	1.27	68 ± 3.8
2-188	64.6	78.9	41.9 ± 3.0	1.63	5.3 ± 0.5	0.9	78 ± 7
2-187[b]	**61.3**	**72.9**					
2-186[b]	**56.6**	**72.7**					
2-184[b]	**43.3**	**-**					

[a] Thermal denaturation of recoverin forms was monitored by tryptophan fluorescence of the protein; $T_{1/2}$, mid-transition temperature.
[b] Recoverin forms with disturbed structural stability were excluded from further testing.
[c] Calcium binding parameters were measured by $^{45}Ca^{2+}$ binding assay.
[d] Binding of recoverin forms to ROS-membranes was measured at different $[Ca^{2+}]_f$ using equilibrium centrifugation assay.
[e] The affinity of recoverin forms to N-RK were studied using SPR spectroscopy. The binding sensorgrams were recorded upon consecutive injections of Ca^{2+}-loaded recoverin forms at increasing concentrations over a sensor-chip surface coated with N-RK via an anti-GST antibody. The equilibrium binding constants (K_D) are based on half-maximal concentration of recoverin required for saturation (Fig. 3C).

TABLE 2

Docking simulations of the interaction of recoverin truncated forms and the RK peptide

Recoverin form[a]	№ of native-like solutions[b]	Ranking of native-like solutions[c]	ZD-s[d]
8-202 (wt)	648 (5.4%)	1; 1; 1	37.68 ± 0.23
8-196	594 (5.0%)	1; 1; 1	37.25 ± 0.23
8-192	596 (5.0%)	1; 1; 1	35.92 ± 0.19
8-190	617 (5.1%)	3; 7; 3	34.71 ± 0.14
8-188	406 (3.4%)	44; 64; 94	33.67 ± 0.14

[a] Recoverin forms used in the simulations, each form starts from residue 8, because the first seven residues were not resolved in the experimental structure (see Methods).
[b] The number of native-like solutions, i.e. with Cα-RMSD < 1 Å with respect to the native complex are reported, out of the 12,000 solutions retained for each recoverin form from three docking runs. In brackets is the percentage of native over total solutions.
[c] The rank of native like-solutions found in each of the three independent docking runs is reported
[d] Average docking score of each cluster of native-like solution ± standard error of the average

Biochemical Journal Immediate Publication. Published on 08 Feb 2011 as manuscript BJ20110013

TABLE 3

The effect of single amino acid substitution in recoverin C-terminal part on the thermal stability of the protein, its calcium binding parameters, Ca^{2+}-dependent interaction with ROS-membranes and the affinity for N-RK

Recoverin form	Thermal denaturation[a]		Binding of calcium[b]		Binding to membranes[c]		Affinity for N-RK[d]
	$T_{1/2}$, °C apo form	$T_{1/2}$, °C Ca^{2+}-bound form	K_D, μM	Hill coefficient	EC_{50}, $[Ca^{2+}]_f$ (μM)	Hill coefficient	K_D, μM
WT	65.1	79.8	19.2 ± 0.4	1.78	3.5 ± 0.2	2.0	10.7 ± 0.6
P190G	64.8	78.1	28.5 ± 1.1	1.45	4.5 ± 0.3	2.0	20.5 ± 1.2
Q191A	65.5	80.8	19.0 ± 0.4	1.39	5.8 ± 0.3	1.5	9.8 ± 0.7
K192A	66.1	81.4	21.9 ± 0.6	1.48	4.9 ± 0.3	2.3	34.1 ± 1.5
V193G	66.5	80.7	20.3 ± 0.8	1.59	4.2 ± 0.3	2.5	28.0 ± 1.6

[a] Thermal denaturation of recoverin forms was monitored by tryptophan fluorescence of the protein; $T_{1/2}$, mid-transition temperature.
[b] Calcium binding parameters were measured by $^{45}Ca^{2+}$ binding assay.
[c] Binding of recoverin forms to ROS-membranes were measured at different $[Ca^{2+}]_f$ using equilibrium centrifugation assay.
[d] The affinity of recoverin forms to N-RK were studied using SPR spectroscopy. The binding sensograms were recorded upon consecutive injections of Ca^{2+}-loaded recoverin forms at increasing concentrations over a sensor-chip surface coated with N-RK via an anti-GST antibody. The equilibrium binding constants (K_D) are based on half-maximal concentration of recoverin required for saturation (Fig. 6B).

Biochemical Journal Immediate Publication. Published on 08 Feb 2011 as manuscript BJ20110013

Figure 1

A

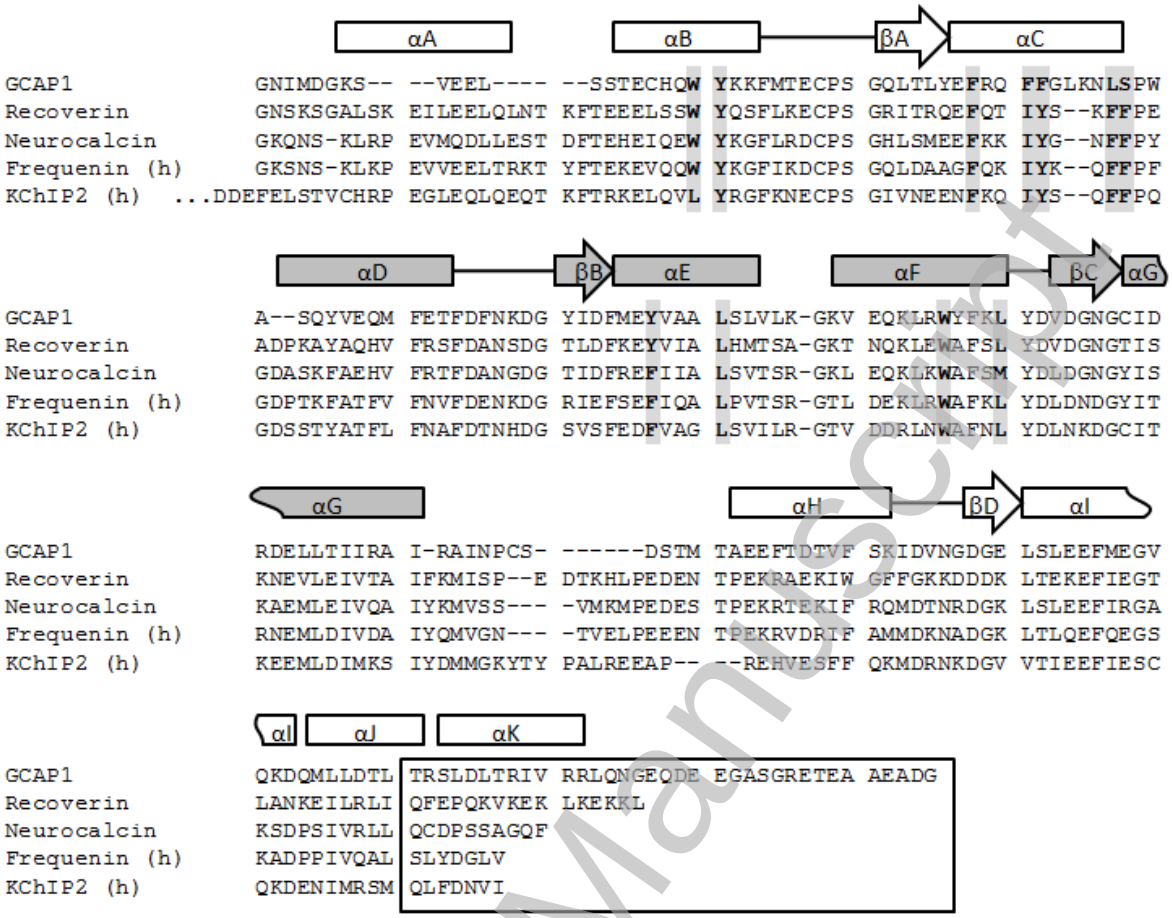

B

Recoverin C-terminus

2-202(wt)	... EILRLI QFEPQKVKEK LKEKKL
2-196	... EILRLI QFEPQKVKEK
2-192	... EILRLI QFEPQK
2-190	... EILRLI QFEP
2-188	... EILRLI QF
2-187	... EILRLI Q
2-186	... EILRLI
2-184	... EILR

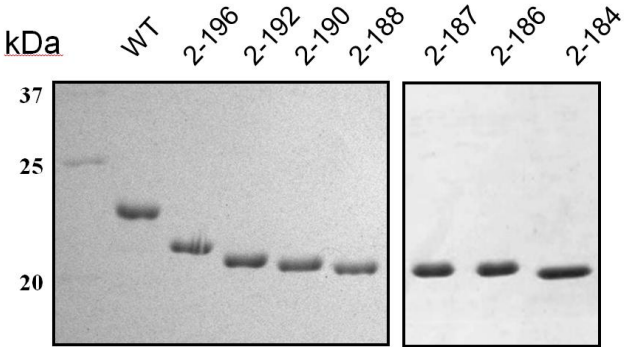

Figure 2

A

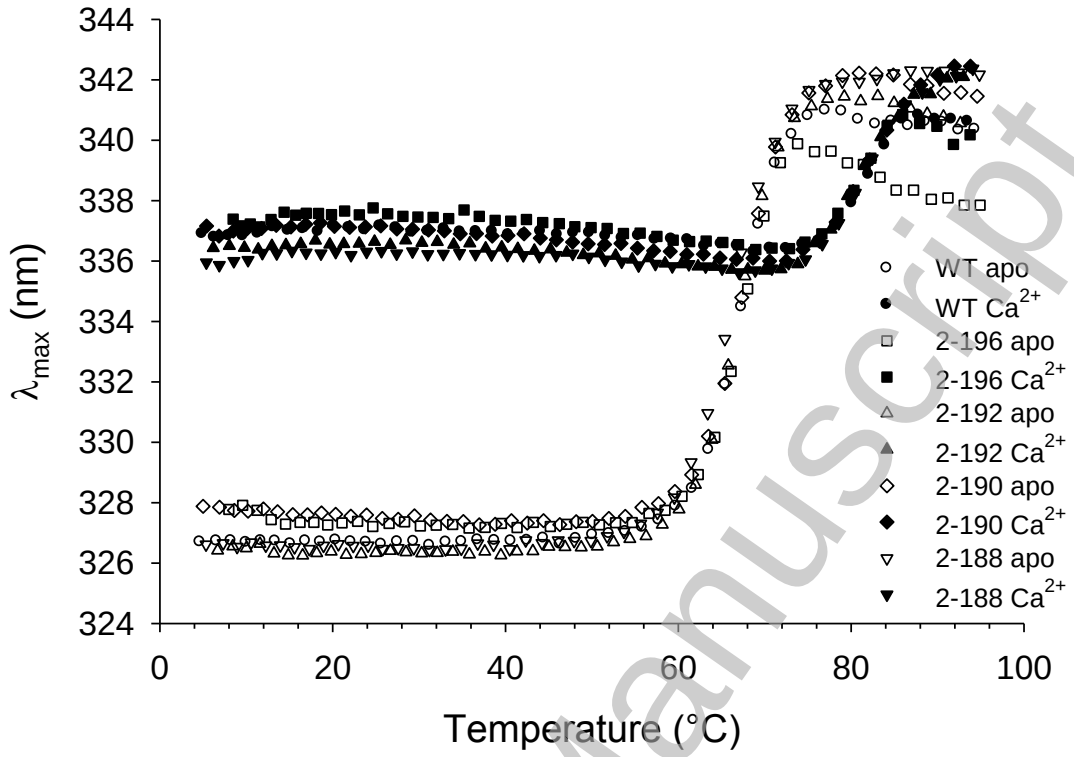

B

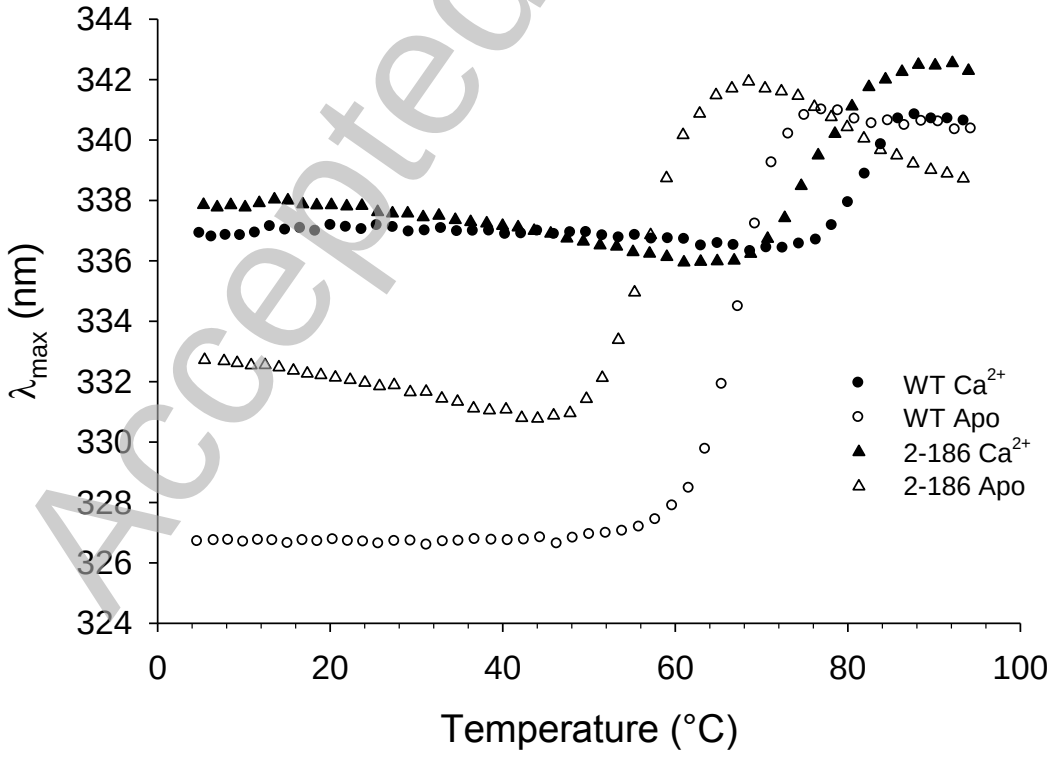

Figure 2

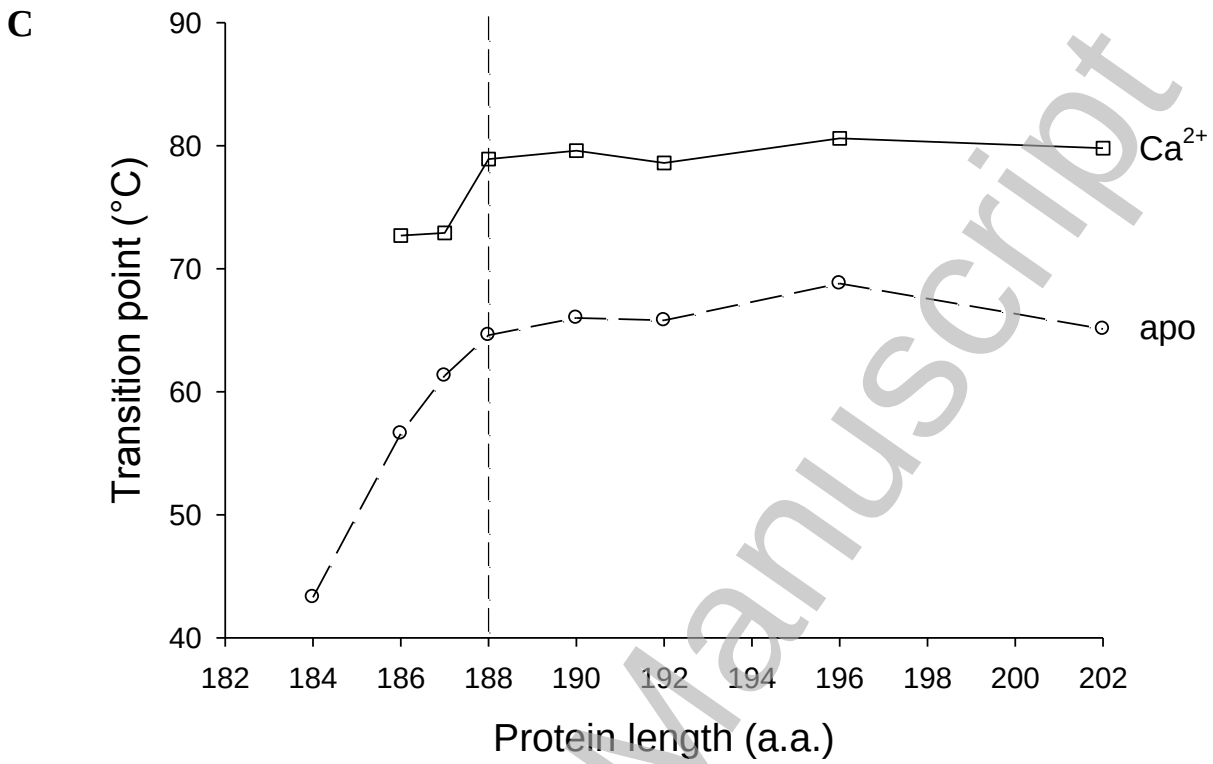

Figure 3

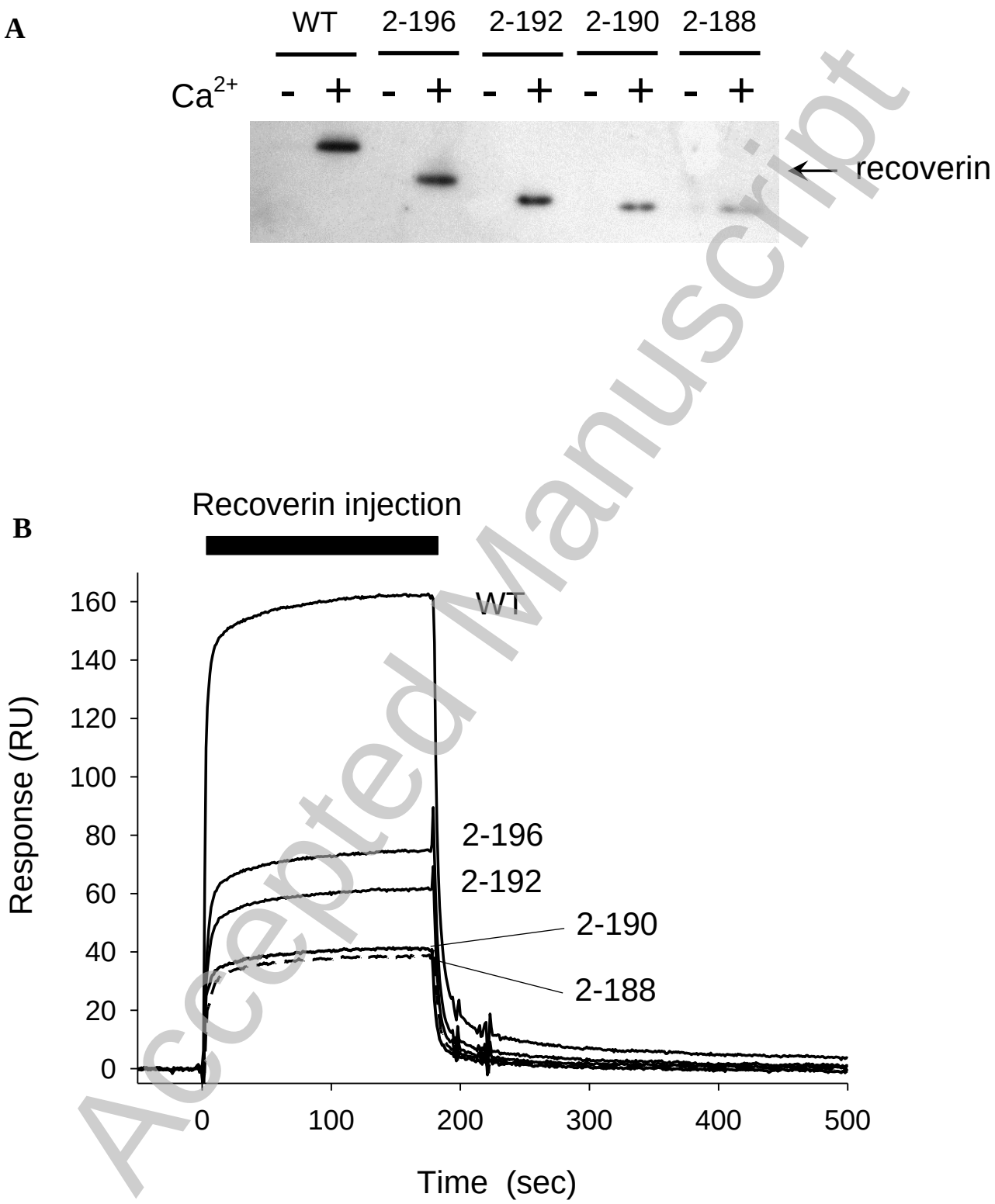

Figure 3

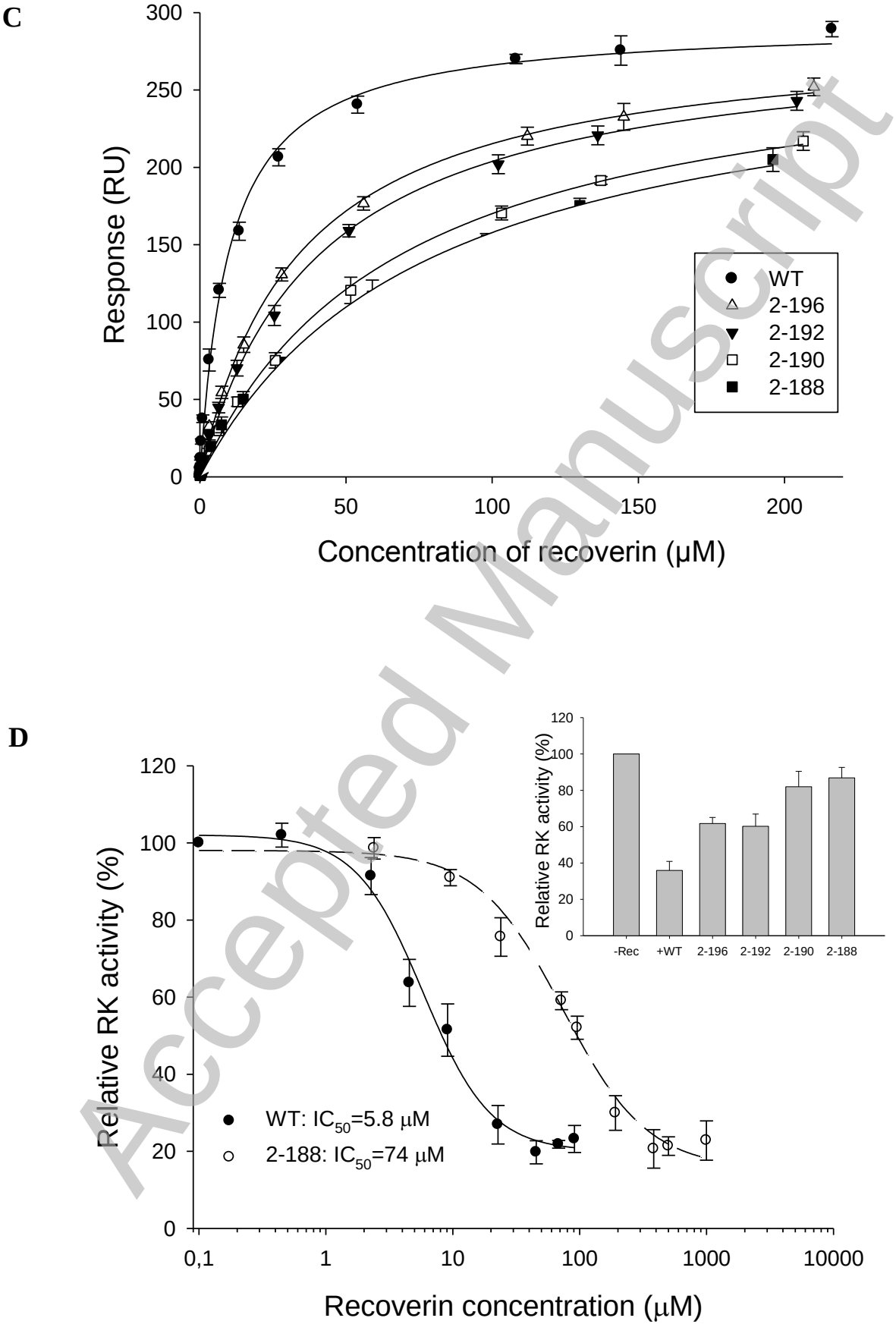

Figure 4

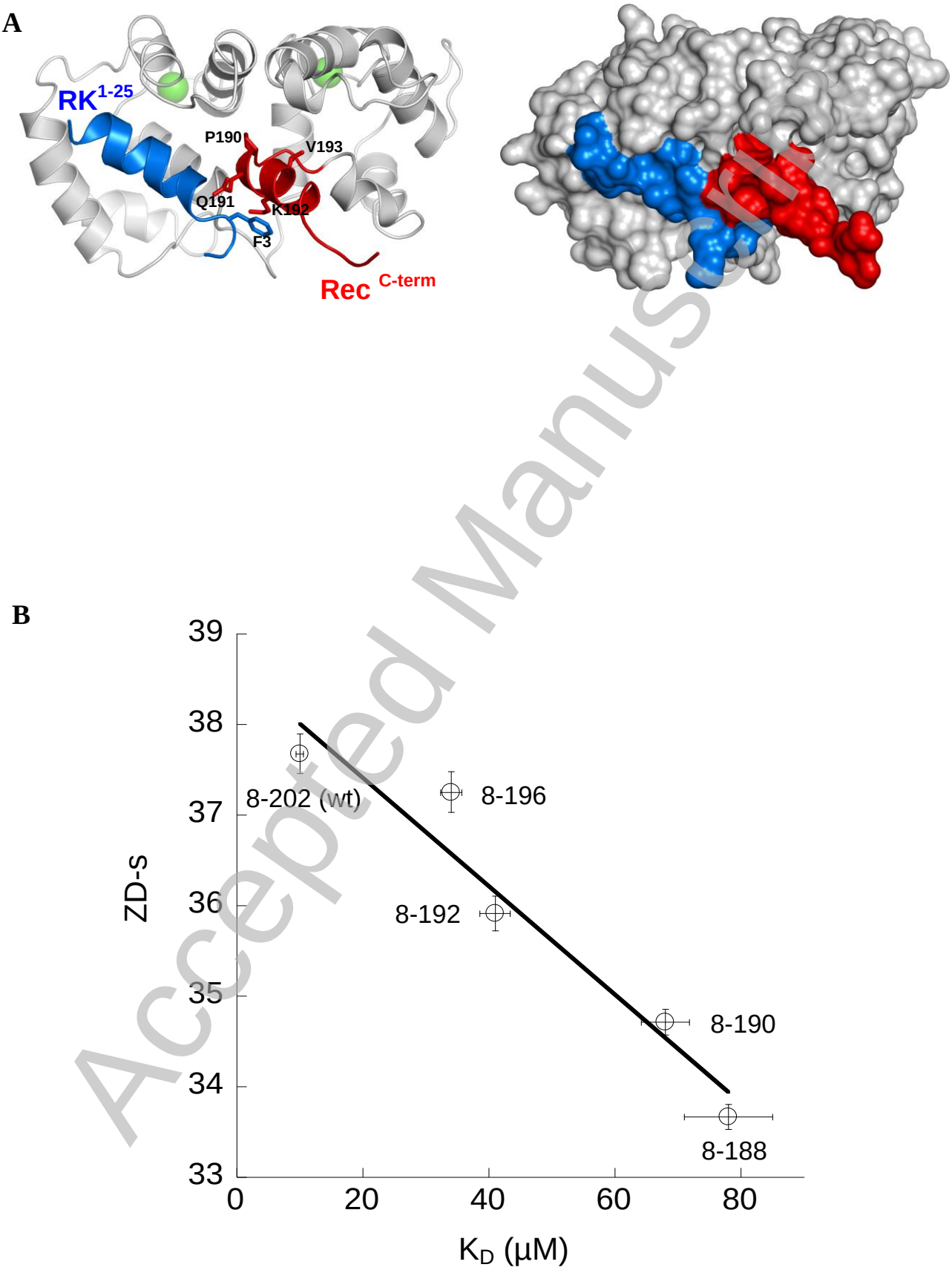

Figure 5

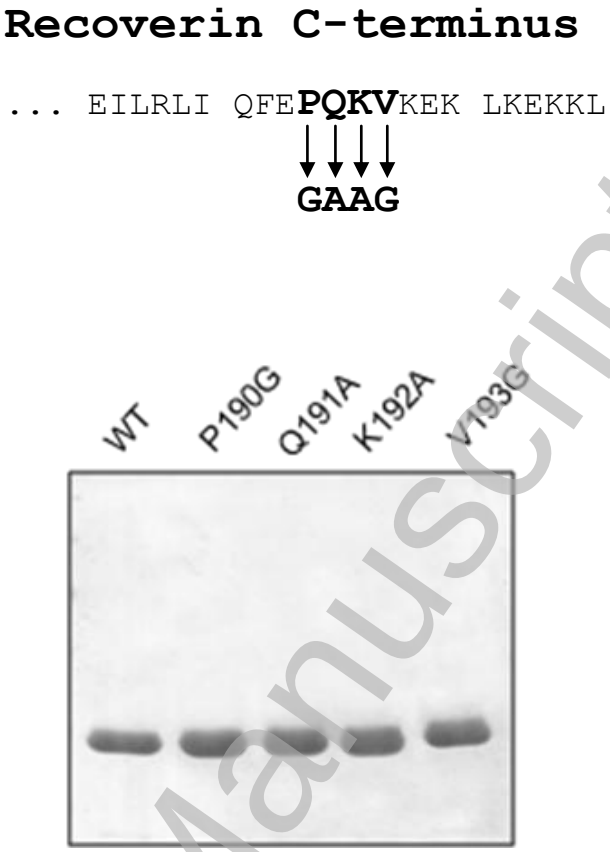

Figure 6

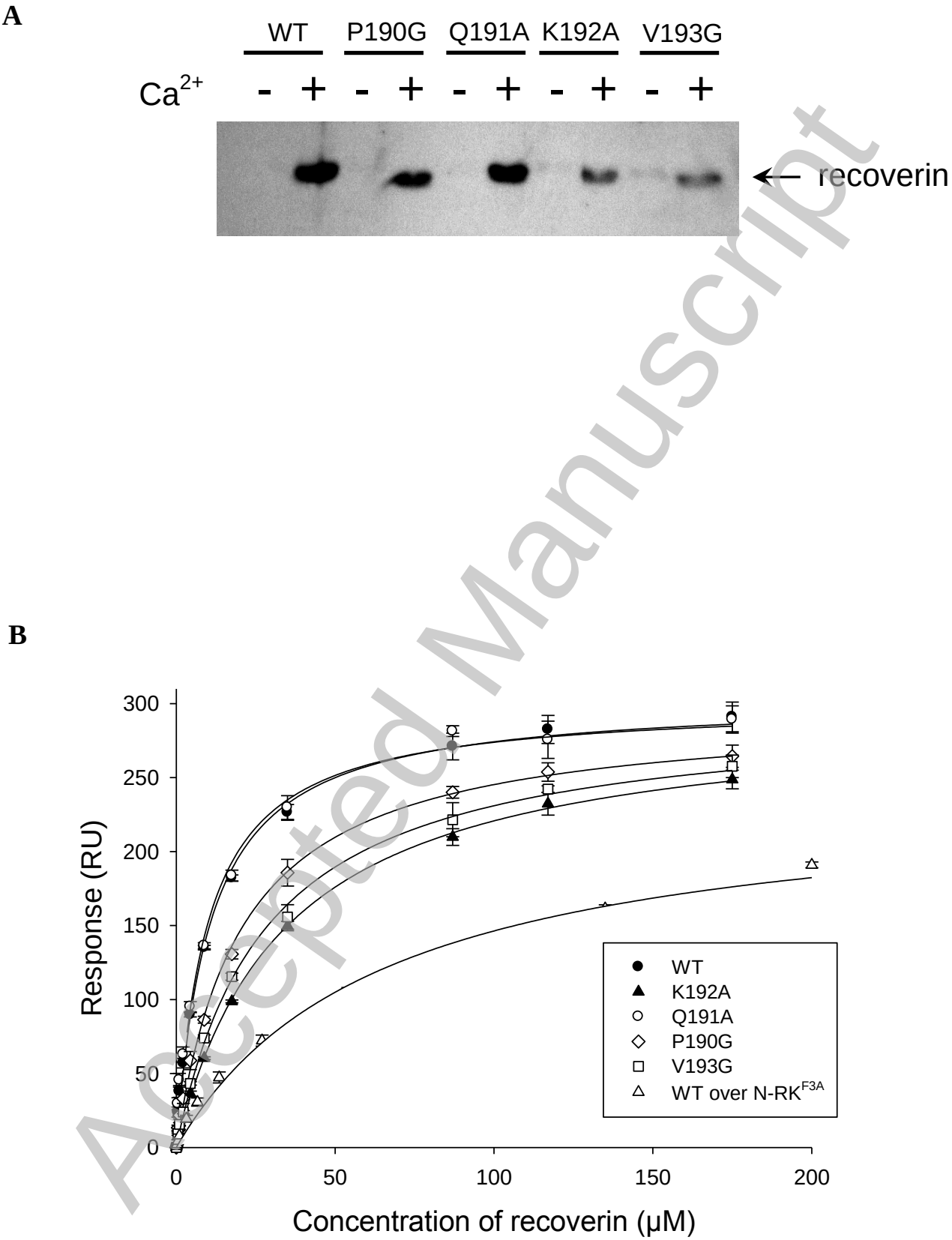

Figure 6

C

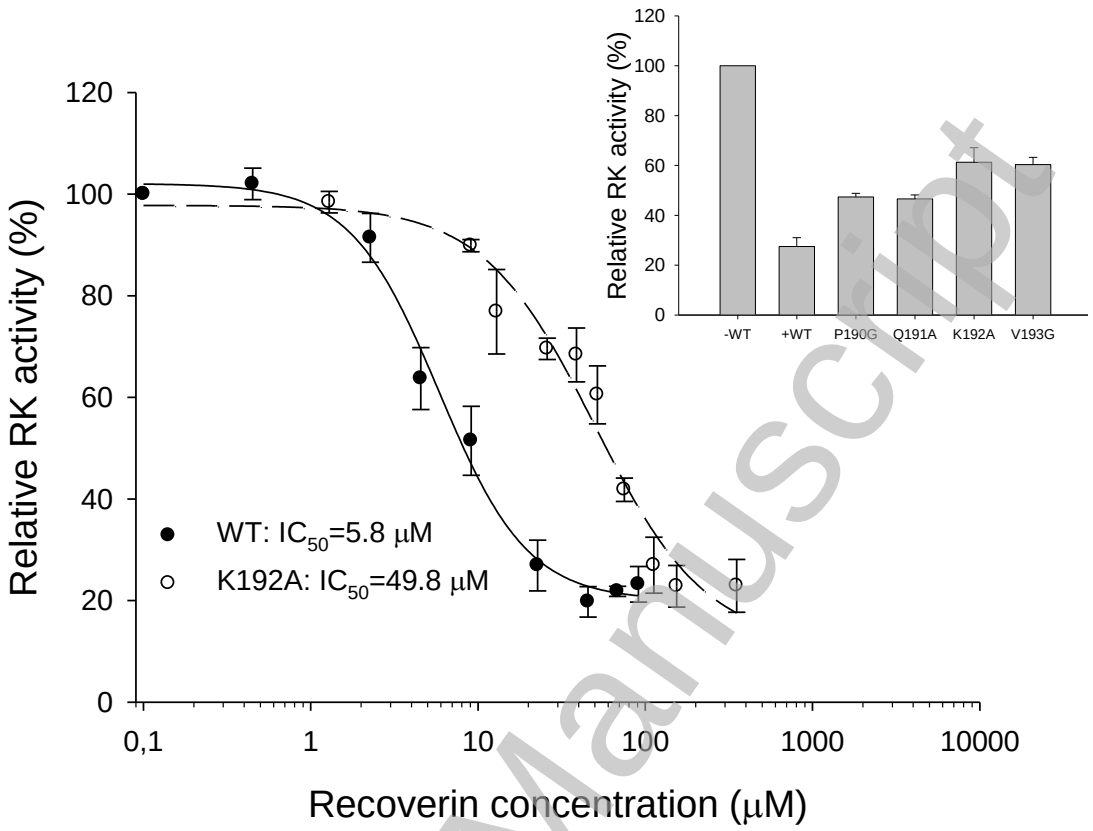

Figure 7